

Water Resources Research®



RESEARCH ARTICLE

10.1029/2023WR034593

Key Points:

- Lab and field data were combined with land-sea modeling to assess growth of a native and an invasive macroalgae under environmental change
- Climate change, urban development, and loss of native forest reduce submarine groundwater discharge to nearshore ecosystems
- Habitat suitability, overall, decreases for the native macroalgae under these changes and increases for the invasive macroalgae

Supporting Information:

Supporting Information may be found in the online version of this article.

Correspondence to:

B. K. Okuhata,
bokuhata@hawaii.edu

Citation:

Okuhata, B. K., Delevaux, J. M. S., Donà, A. R., Smith, C. M., Gibson, V. L., Dulai, H., et al. (2023). Effects of multiple drivers of environmental change on native and invasive macroalgae in nearshore groundwater dependent ecosystems. *Water Resources Research*, 59, e2023WR034593. <https://doi.org/10.1029/2023WR034593>

Received 1 FEB 2023

Accepted 10 JUL 2023

Author Contributions:

Conceptualization: B. K. Okuhata, C. M. Smith, H. Dulai, K. M. Burnett, L. L. Bremer

Data curation: B. K. Okuhata, J. M. S. Delevaux, A. Richards Donà, C. M. Smith, H. Dulai, L. L. Bremer

Formal analysis: B. K. Okuhata, J. M. S. Delevaux, A. Richards Donà, C. M. Smith, L. L. Bremer

Funding acquisition: C. M. Smith, H. Dulai, A. I. El-Kadi, K. M. Burnett, L. L. Bremer

© 2023. The Authors.

This is an open access article under the terms of the [Creative Commons Attribution License](https://creativecommons.org/licenses/by/4.0/), which permits use, distribution and reproduction in any medium, provided the original work is properly cited.

Effects of Multiple Drivers of Environmental Change on Native and Invasive Macroalgae in Nearshore Groundwater Dependent Ecosystems

B. K. Okuhata^{1,2} , J. M. S. Delevaux^{3,4,5}, A. Richards Donà^{1,6} , C. M. Smith⁶ , V. L. Gibson^{1,6}, H. Dulai^{1,2} , A. I. El-Kadi^{1,2}, K. Stamoulis⁵, K. M. Burnett⁴, C. A. Wada⁴, and L. L. Bremer^{1,4} 

¹Water Resources Research Center, University of Hawai'i at Mānoa, Honolulu, HI, USA, ²Department of Earth Sciences, University of Hawai'i at Mānoa, Honolulu, HI, USA, ³The Natural Capital Project, Stanford University, Stanford, CA, USA, ⁴University of Hawai'i Economic Research Organization, Honolulu, HI, USA, ⁵Seascape Solutions LLC, Mililani, HI, USA, ⁶School of Life Sciences, University of Hawai'i at Mānoa, Honolulu, HI, USA

Abstract Groundwater dependent ecosystems (GDE) are increasingly recognized as critical components of sustainable groundwater management, but are threatened by multiple drivers of environmental change. Despite this importance, data that link drivers of hydrologic change to GDEs are scarce. This study adapts a land-sea modeling framework by calibrating marine models with macroalgal experiments to quantitatively assess impacts of climate and land use change on submarine groundwater discharge (SGD) and subsequent habitat suitability for a native (*Ulva lactuca*) and an invasive (*Hypnea musciformis*) macroalgae in nearshore GDEs in Kona, Hawai'i. Lab analyses demonstrate that while *U. lactuca* grows optimally in low-salinity, high-nutrient waters, *H. musciformis* appears constrained to a salinity threshold and exhibits low growth in low salinity despite high nutrient concentrations. Land-sea model results predict that while a dry future climate (Representative Concentration Pathway 8.5 mid-century) coupled with increased urban development will likely reduce SGD, protecting native forests may prevent further loss of SGD quantity. This prevention thus partially mitigates the decline in habitat suitability of *U. lactuca* due to the combined effects of climate and land use change. Findings also suggest that, in contrast to the native *U. lactuca*, reductions in SGD may favor *H. musciformis* growth if introduced to Kona. Collectively, this study demonstrates the importance of considering multiple drivers of environmental change on GDEs. This study bridges experiments with models to spatially map changes in species abundance beyond their current habitat conditions, and thus informs management actions that can explicitly incorporate future human and climate-related impacts.

1. Introduction

There is a growing global need to incorporate the protection and restoration of groundwater dependent ecosystems (GDEs) into groundwater management and policy (Burnett et al., 2020; Elshall et al., 2020; Kløve et al., 2014; Rohde et al., 2017; Wada et al., 2020). GDEs encompass a wide range of systems, including anchialine pools, coastal springs, water caves, indigenous aquaculture systems, and coral reefs, which all often have high cultural and ecological value (Eamus & Froend, 2006; Gibson et al., 2022). Although varied, these systems are highly adapted to and dependent on low-salinity and optimal-nutrient subsidies from submarine groundwater discharge (SGD; Cantonati et al., 2020; Dulai et al., 2021). Via this “invisible pathway,” SGD transports terrestrial groundwater to the coastline in both diffuse and discrete (point source) manners (e.g., Duarte et al., 2010; Taniguchi et al., 2019). The quantity and quality of the SGD that flow into these GDEs, however, is impacted by multiple interacting drivers of environmental change (Boulton, 2020; Dulai et al., 2021; Taniguchi et al., 2019). Threats from climate change and land use on water resources have great potential to rapidly affect GDEs, especially in hydrologically permeable settings with shallow coastal aquifers like the Hawaiian Islands and other Pacific Islands (Nunn et al., 2016).

As an important component of nearshore ecosystems, diverse marine macroalgae are conspicuous indicators of GDE health (Duarte et al., 2010). In extreme cases when nutrient inputs are elevated to unsuitable levels (associated with land-based sources of pollution such as wastewater mismanagement and excessive agricultural inputs), invasive growth blooms can occur (Amato et al., 2018, 2020; Dailer et al., 2010; Smith et al., 2002). These growth blooms can have deleterious effects on GDEs and their associated native species, and often smother coral reefs (Conklin & Smith, 2005; Smith et al., 2002). This can lead to the deterioration of a reef's structure,

Investigation: B. K. Okuhata, J. M. S. Delevaux, A. Richards Donà, C. M. Smith, L. L. Bremer
Methodology: B. K. Okuhata, J. M. S. Delevaux, A. Richards Donà, C. M. Smith, V. L. Gibson, H. Dulai, A. I. El-Kadi, K. Stamoulis, K. M. Burnett, C. A. Wada, L. L. Bremer
Project Administration: L. L. Bremer
Resources: C. M. Smith, H. Dulai, A. I. El-Kadi, L. L. Bremer
Software: B. K. Okuhata, J. M. S. Delevaux, A. I. El-Kadi
Supervision: L. L. Bremer
Validation: B. K. Okuhata, J. M. S. Delevaux, A. Richards Donà, C. M. Smith, L. L. Bremer
Visualization: B. K. Okuhata, J. M. S. Delevaux, A. Richards Donà
Writing – original draft: B. K. Okuhata, J. M. S. Delevaux, A. Richards Donà, L. L. Bremer
Writing – review & editing: B. K. Okuhata, J. M. S. Delevaux, A. Richards Donà, C. M. Smith, V. L. Gibson, H. Dulai, A. I. El-Kadi, K. Stamoulis, K. M. Burnett, C. A. Wada, L. L. Bremer

resulting in a further loss of biodiversity (e.g., Lapointe, 1997; Rosado-Torres et al., 2019). Although a majority of macroalgae species are intolerant of freshwater (Dulai et al., 2021), some native species are highly adapted to low salinity and elevated nutrients associated with SGD (Amato et al., 2018; Dulai et al., 2021; Huisman et al., 2007). The complex integration of both nutrients (bottom-up control; resource availability) and herbivores (top-down control; predator actions) plays an important role in coastal ecosystems (Littler et al., 2006; Smith et al., 2001, 2010) as coastal waters experience near continuous eutrophication while herbivorous fish stocks are in historic decline. Many coastal communities are forced to seek mitigation for these negative effects of changing land use and sources of pollution. Invasive algal blooms have been seen across the world in, for example, Florida, Jamaica, and Bermuda (e.g., Bell, 1992; Lapointe, 1997; Lapointe & O'Connell, 1989). Most of these regions are heavily influenced by SGD, which transports anthropogenic nutrient-enriched waters to the coastline, allowing algae to grow rapidly.

In Hawai'i, native algal species (known in the Hawaiian language as *limu*), such as *Ulva lactuca* (*limu pālahalaha*), inhabit SGD-influenced systems (Amato et al., 2016; Huisman et al., 2007), have high cultural value as traditional food sources (Abbott, 1978; Abbott & Shimazu, 1985; Abbott & Williamson, 1974; Duarte et al., 2010), and are commonly eaten by native fish (S. Chulakote, personal communication, 27 September 2022). Invasive algal species, such as *Hypnea musciformis*, however, threaten native species by smothering healthy coastal ecosystems. For example, blooms of these co-occurring species on Maui have resulted in an estimated \$20 million per annum cost in lost revenue (Dailer et al., 2010; Smith et al., 2002; Van Beukering & Cesar, 2004). This study therefore seeks to directly test and better understand the potential role of nutrient-rich SGD conditions in facilitating (or preventing) the invasion of Kona by the well-known, highly invasive, *H. musciformis* (Williams & Smith, 2007). Changes in SGD quantity and quality can modify conditions to favor invasive algae growth, which may cause significant disturbances to GDEs (Dailer et al., 2010; Stamoulis et al., 2017). With the social-ecological importance of GDEs coupled with increasing development pressure and a drying climate (Elison Timm et al., 2015; Fukunaga & Associates, Inc., 2017; Gibson et al., 2022), the Keauhou aquifer, located on the west coast of Hawai'i Island, has become a pertinent aquifer when discussing how water and land management influence these important resources.

This work combines lab and field data with stacked land-sea modeling to assess the combined impact of salinity, nutrients, and temperature on the growth and distribution of two important macroalgae species—the culturally and ecologically important *U. lactuca* and the broadly distributed, highly invasive *H. musciformis*. Typically, species distribution models use field data to calibrate, predict, and validate the range of current species occurrence. This, however, impedes the study's ability to extrapolate species distribution to environmental conditions outside those within the sample space and time (Elith & Leathwick, 2013). This work, therefore, assesses the possibility of *H. musciformis* invasion beyond its current distributional range by leveraging lab data to predict where this invasive species can potentially settle and increase along the Kona coastline if introduced to Hawai'i Island.

In this study, a ridge-to-reef framework (Delevaux et al., 2018) is adapted to the Keauhou aquifer as an archetype system to examine how environmental drivers, impacted by climate change and human activities, may influence SGD quantity and quality, and links these drivers to the growth distribution of macroalgae. Specifically, we assess: (a) the relative influence of a dry future climate (Representative Concentration Pathway (RCP) 8.5 mid-century), future urban development, and native forest conversion scenarios on nearshore water quality; and (b) how these changes could impact the spatial distribution and abundance of *U. lactuca* and *H. musciformis*. In sum, this novel study expands the predictive range of a land-sea modeling framework by using manipulative lab experiments, validated with field data, to forecast the impact of land use and climate change on both culturally important and highly invasive algal species in tropical environments. This study exemplifies stakeholder-driven science aimed to highlight and protect GDEs in the context of the public trust doctrine in Hawai'i. Various resource managers are now working to better understand the links between changes in water quality, quantity and GDE health, including use of indicator algal species (Adler & Ranney, 2018).

2. Materials and Methods

2.1. Study Site

The Keauhou aquifer (426 km²) is located in the north Kona district on the western coast of Hawai'i Island, and encompasses the southern flank of Hualālai volcano (Figure 1a). The Keauhou aquifer is hydrogeologically complex, where groundwater occurs as a thin freshwater lens near the coast and a high-level aquifer located approximately 6 km inland (e.g., Fackrell et al., 2020; Oki, 1999; Okuhata et al., 2021). A hydrogeologic structure,

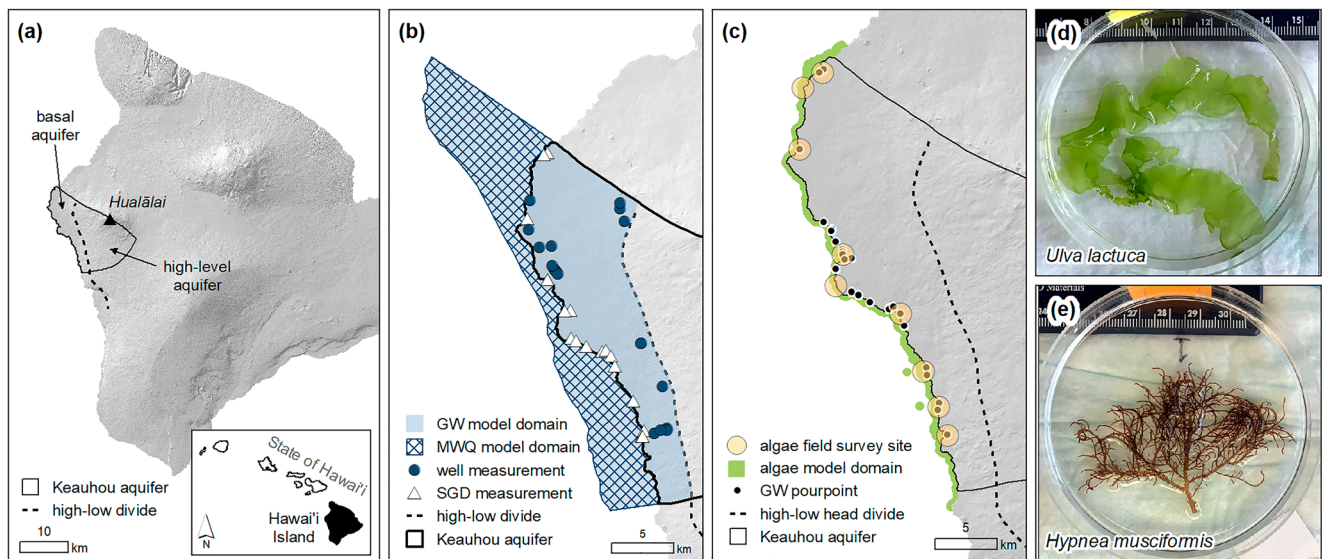


Figure 1. (a) Study site area; (b) Groundwater (GW) and marine water quality (MWQ) model domains and measured calibration points; (c) GW pourpoints, locations of nine algae survey sites in relation to SGD plumes, and algae model domain; (d) *Ulva lactuca* sample; (e) *Hypnea musciformis* sample.

referred to as the high-low head divide, is believed to exist within the subsurface and provides a partial barrier for groundwater flow from the high-level aquifer to the basal lens (Oki, 1999). The thin freshwater lens, referred to as the basal aquifer (150 km²), is characterized by low head levels and is thought to be fed by local recharge and groundwater flow from the high-level aquifer. The basal lens feeds numerous coastal brackish SGD springs (Figure 1b) which have varying discharge rates that range from a few hundred to thousands of cubic meters per day. The locations and approximate discharge rates of the SGD springs were previously determined by Johnson et al. (2008) using aerial thermal infrared imagery in combination with geochemical tracer quantification of SGD.

Downstream, the dominant benthic substrate is narrow fringing reefs, with generally high coral cover due to low wave action (Delevaux et al., 2018; Smith et al., 2016). The nearshore coast of Kona comprises a reef region, where biota are particularly well represented with large areas of aggregated coral and colonized volcanic rocks with boulders (Analytical Laboratories of Hawai'i, no date). Large regions of sandy substrate and smaller areas with native seagrass also form major habitat types. Macroalgal growth along the Kona coast is most common in the rocky intertidal zone (Figure 1c) where herbivory is limited by wave action or geologic barriers (i.e., cliffs, tidepools). Along the Keauhou coastline (and across the State of Hawai'i), a native algae, *U. lactuca* (Figure 1d), is a dominant constituent of the algal community, particularly near SGD springs. Comparatively, the aggressive invasive species, *H. musciformis* (Figure 1e; Williams & Smith, 2007), is not currently found on Hawai'i Island (Smith et al., 2002), but may have a devastating impact on the native algae and coral distributions if it were to spread from the nearby island, Maui. Below the tide line and outside the protected tide pools, most macroalgal growth is controlled by herbivore pressure and limited nutrients (Smith et al., 2001), thus herbivore resistant turf and crustose algal forms are more commonly observed in deeper waters.

The Keauhou aquifer, particularly land area overlying the upland high-level aquifer, contains large tracts of native forest, much of which is threatened by higher-water-use invasive plant species or by conversion to non-native grasslands through overgrazing or fire (Bremer et al., 2021). Given the importance of watershed management for groundwater resources and biodiversity conservation, a number of conservation organizations work to protect these native forests. Recently, the Hawai'i Department of Water Supply commissioned a study to evaluate the areas where watershed protection strategies would yield the most benefits for groundwater recharge. It was found that over 50 years, forest protection could save up to 6.1 million m³ of fresh water across the Keauhou and Kealakekua aquifers (Bremer et al., 2021). Additionally, development in the region overlying the coastal Keauhou aquifer is continuously expanding, where approximately 28% of the land is currently classified as urban development and approximately 38.4 km² of land has been granted permits for future development (Fukunaga & Associates, Inc., 2017; National Oceanic and Atmospheric Administration, 2006).

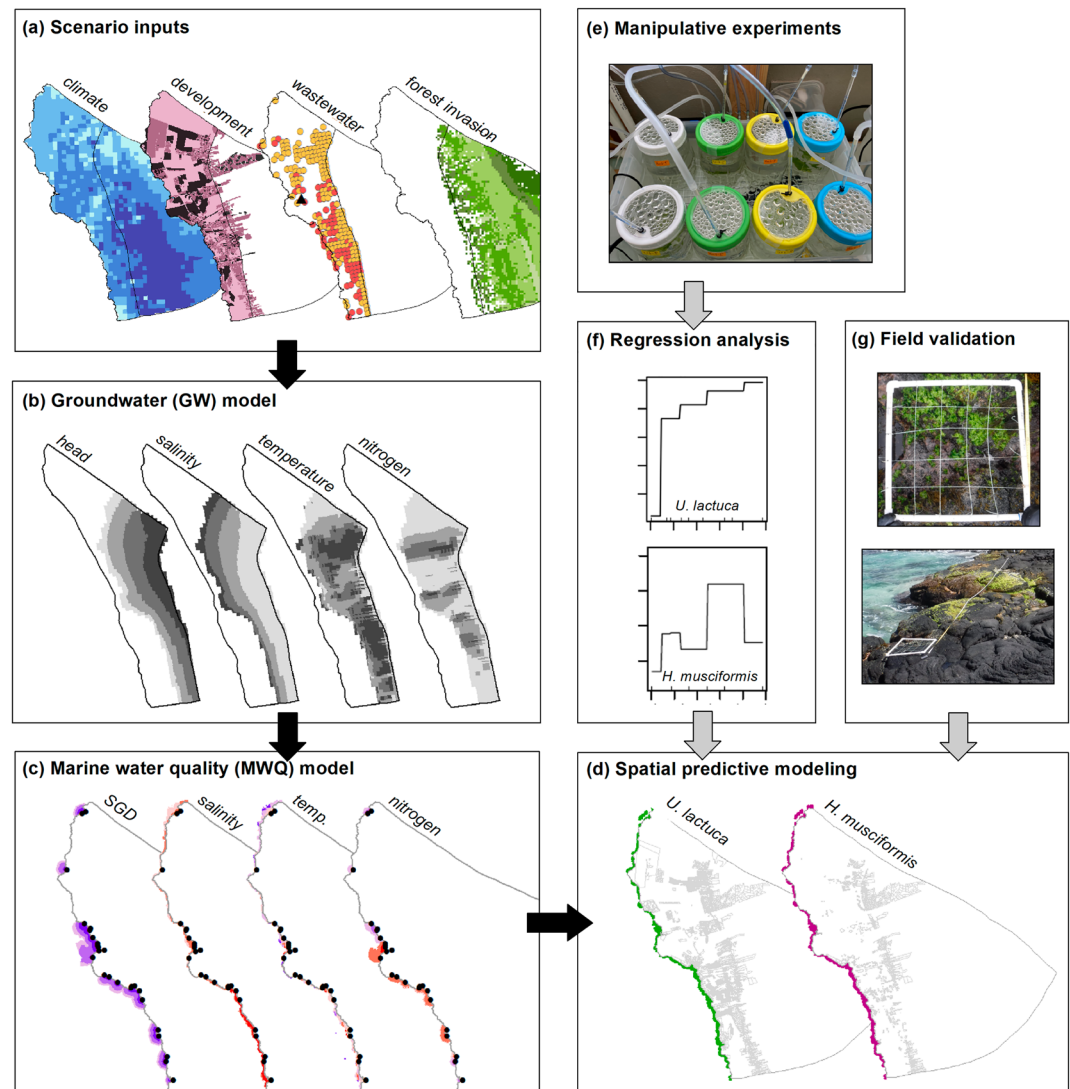


Figure 2. Overview of the parallel work streams (black vs. gray arrows) of the adapted ridge-to-reef framework. (a) Scenario coverages were applied to the baseline models to yield (b) groundwater and (c) marine water quality results and (d) predict the spatial distribution of *U. lactuca* and *H. musciformis* under the various scenario assumptions. (e) Manipulative algal growth experiments were used to characterize the (f) regression models, which were used to (d) predict the spatial distribution of *U. lactuca* and *H. musciformis*. (g) Field surveys were used to validate the modeled distribution of *U. lactuca*.

2.2. Project Framework

This study adapted and applied a ridge-to-reef framework (Delevaux et al., 2018), which follows two parallel workflows that combine groundwater (GW), marine water quality (MWQ), and marine biomass predictive models to assess the impact of management scenarios. In the first workflow (following the black arrows in Figure 2), land use and climate change scenarios pertinent to this study area were developed to examine potential futures for climate, urban development, and native forest protection (further described in Section 2.3). These scenarios were applied to a previously developed groundwater model (Okuhata et al., 2021) to simulate groundwater flow, salinity, temperature, and nutrient concentrations, which were diffused at the coast with depth and wave power to generate MWQ results for each new management scenario.

In the second workflow (following the gray arrows in Figure 2), the framework was augmented by designing lab-based manipulative algal growth experiments to calibrate a new marine spatial predictive model. The spatial predictive model was then used to characterize the response of *U. lactuca* and *H. musciformis* biomass to change in SGD conditions (i.e., nutrients, salinity, and temperature) and predict the range of suitable habitat along the

Table 1
Generalized Descriptions of Each Modeled Scenario

#	Scenario name	Climate	Development	Forest
0	Baseline	Current climate	Current development	Existing native forest
1	Climate change	Future (RCP 8.5 mid-century)	Current development	Existing native forest
2	Urban development	Future (RCP 8.5 mid-century)	Permitted development ^a	Existing native forest
3	Native forest conversion + Urban development	Future (RCP 8.5 mid century)	Permitted development ^a	Forest invasion

^aPermitted development includes an increase in wastewater effluent that is assumed to be treated in the Kealahou Wastewater Treatment Plant.

Keauhou coast as a result of the study-pertinent scenarios. Field surveys were used to ground-truth the current modeled distribution of *U. lactuca* and to gain confidence while extrapolating the lab data to the modeled change in *U. lactuca* and *H. musciformis* distribution.

2.3. Climate and Land Use Change Scenarios

Future scenarios developed for this study aim to project the relative influence of climate change, urban development, and native forest conversion on groundwater quantity and quality, coastal water quality, and algal growth and spatial distribution (Table 1). The urban development and native forest protection scenarios were co-developed with land and water management stakeholders in the Kona region (see Bremer et al., 2021; Wada et al., 2021).

Scenario 0 (Baseline) assumes current land use (; State of Hawai'i, 2022) combined with the most up-to-date groundwater recharge conditions (1984–2008 period; Engott, 2011) and groundwater withdrawal rates (1990–2017; Commission on Water Resource Management, unpublished data, 2018). See Okuhata et al. (2021) for full description of the baseline groundwater model scenario.

Scenario 1 (Climate Change) assumes current land use with a dry future climate (RCP 8.5 mid-century rainfall projections; Elison Timm et al., 2015). Future groundwater recharge was calculated as:

$$G_F = (R_C - R_F) \times 0.45 + G_C \quad (1)$$

where G_F = future groundwater recharge, R_C = current rainfall (Giambelluca et al., 2013), R_F = future rainfall (RCP 8.5 mid-century; Giambelluca et al., 2013), and G_C = current groundwater recharge. The change in rainfall is translated to recharge using the USGS recharge to rainfall ratio (0.45) for the Keauhou aquifer (Engott, 2011). Although RCP 8.5 was initially considered an extreme scenario, we are already projected to overshoot this scenario based on current emissions (Schwalm et al., 2020). As such, the baseline climate is used as a low-range potential future climate and RCP 8.5 mid-century as a mid-to upper-range climate projection.

Scenario 2 (Urban Development) assumes RCP 8.5 mid-century rainfall conditions (as in Scenario 1), but also evaluates the impact of future permitted development (which includes an increased water demand of 64,080 m³/d (Fukunaga & Associates, Inc., 2017)). Under this scenario, it is assumed that existing native forests within the Keauhou aquifer, which have substantial fog interception, are protected from the invasion of either higher-water-use canopy species or from conversion to non-native grassland areas.

Scenario 3 (Native Forest Conversion + Urban Development) assumes RCP 8.5 mid-century rainfall conditions and future permitted development (as in Scenario 2), but assumes that native forests are not protected. Under this scenario, non-native forests are assumed to expand at a 5% rate in lower elevation areas, and non-native grasslands are assumed to expand at a 2% rate in higher elevation areas (Bremer et al., 2021). While ecohydrology data are limited in Hawai'i, available data suggests that a typical invasive canopy species (strawberry guava; *Psidium cattleianum*) have higher evapotranspiration rates than a typical native forest species ('Ōhia lehua; *Metrosideros polymorpha*) (Giambelluca et al., 2014), and that forests capture more fog drip than grasslands in areas above ~760 m elevation (Engott, 2011). These land cover changes were translated into recharge using a water balance approach where the avoided loss of freshwater yield was modeled as the sum of the avoided increase in actual evapotranspiration (AET) and the avoided loss of fog interception. AET without forest protection used a regression approach (Wada et al., 2017), which includes a large spatial dataset of current annual AET and a series of climatic and vegetation predictor variables across Hawai'i Island. Changes in fog interception above ~760 m were modeled following Engott (2011) (see Supporting Information S1 – Section 1).

2.4. Groundwater Model Development

This study used a three-dimensional, density-dependent, multi-species numerical groundwater model previously developed by Okuhata et al. (2021) using the program SEAWAT (Langevin et al., 2008), which ran in transient mode. The new climate and land use change scenarios pertinent to this study were applied to the groundwater model to simulate groundwater flow, salinity, temperature, and nutrient concentrations, which served as the foundation of the first project workflow. Specific details regarding model development can be found in Okuhata et al. (2021) and Wada et al. (2021). Briefly, the model domain spans across the basal Keauhou aquifer and further offshore, with a top elevation that follows topography and bathymetry, and a bottom elevation of 550 m below msl. For this particular study, the model grid was refined around coastal spring locations for better accuracy (107,991 cells total). The horizontal span of the grid cells therefore range from 40 to 490 m.

The top of the inland model domain was assigned recharge values based on the USGS Hawai'i Island water budget model (Engott, 2011). The ocean floor was assigned a general head (i.e., head dependent) boundary condition with a conductance of $1 \text{ m}^2/\text{d}/\text{m}^2$ and salinity of 35 ppt (Okuhata et al., 2021). Coastal springs were simulated as point drains (i.e., head-dependent sinks) and therefore assigned conductance values proportional to measured discharge rates (Okuhata et al., 2021). The top two layers of the eastern model boundary were assigned a specified flow value of $388,399 \text{ m}^3/\text{d}$ to represent groundwater flux from the high-level aquifer. This value was determined based on recharge calculations from Engott (2011) and also considers the reported volume of groundwater withdrawn from high-level pumping wells ($16,310 \text{ m}^3/\text{d}$) to accommodate the current water demand (Commission on Water Resource Management, unpublished data, 2018). The specified flow assigned to the eastern boundary condition for each scenario considered the increased pumping to account for future water demands ($64,080 \text{ m}^3/\text{d}$) as well as the reduced recharge from the upland Keauhou aquifer according to climate change and forest protection assumptions. This boundary condition was also assigned salinity, nitrogen (N) and phosphorus (P) concentrations of 0.26 ppt, 1.0 mg/L, and 0.1 mg/L, respectively, based on high-level aquifer well measurements (Okuhata et al., 2021). The flux concentrations were held constant for all scenarios.

Land use was divided into three main categories: natural background (including forests, shrublands and pastures), golf courses (State of Hawai'i, 2022), and urban development, which was further divided into three intensity levels (low, medium, high;). Each land use category and intensity level was assigned an annual recharge nutrient concentration (refer to Table 1 in Okuhata et al., 2021). The Kealahou Wastewater Treatment Plant (WWTP) currently receives approximately $6,400 \text{ m}^3$ of sewage per day, which is treated and disposed into a percolation basin that eventually discharges into the ocean (e.g., Wilson Okamoto Corporation, 2019; Wada et al., 2021). There are approximately 7,400 onsite sewage disposal system (OSDS) units installed within the study area, and 84% of those units are cesspools (State of Hawai'i, 2022; Whittier & El-Kadi, 2014). On average, N and P concentrations are 60.5 mg/L and 16.5 mg/L, respectively, in wastewater effluent released from cesspools (Whittier & El-Kadi, 2009). Further details regarding land use, development, and wastewater infrastructure can be found in Supporting Information S1 - Section 1.

The model includes 35 pumping wells with average withdrawal rates that range from six to $17,000 \text{ m}^3/\text{d}$. Pumping rates were documented from 1990 to 2017 and obtained from the State of Hawai'i's Commission on Water Resource Management (CWRM). The model was calibrated with 54 water levels from wells measured by CWRM between 1944 and 2008. Salinity, N and P concentrations were calibrated with 20 well measurements (Tachera, 2021) and 13 SGD plume measurements (H. Dulai, University of Hawai'i at Mānoa, unpublished data, 2019) (Figure 1b). The model was further calibrated using two years (12/1/2019—2/28/2021) of tidal data from the Kawaihae station (National Oceanic and Atmospheric Administration, 2021). Simulated transient salinities were calibrated against transient salinities measurements collected during the same time period (H. Dulai, University of Hawai'i at Mānoa, unpublished data, 2021). It is important to note that the measured coastal conditions were obtained from a single SGD plume location, and therefore is not representative of all plume conditions, thus explaining some of the observed mismatch. This is most notable with the temperature calibrations, particularly in areas surrounding the Kealahou WWTP, where the wastewater likely influences measured temperatures. The simulated and measured results can be found in Supporting Information S1—Section 2. An additional identical numerical model was used to simulate groundwater temperatures. Based on ocean water samples, the nearshore ocean floor boundary was assigned a temperature of 27°C . The OSDS and WWTP points were assigned a typical wastewater temperature of 25°C (Babcock et al., 2004). Recharge was assigned a temperature of 22°C based on groundwater measurements sampled near the water table, and the eastern boundary condition was assigned a

temperature of 21°C based on average temperatures measured from high-level pumping wells. To aid in reducing computational expense, salinity was the only other parameter assigned to this temperature model, which served as an additional calibration parameter and common factor to integrate the two simulated models.

2.5. Marine Water Quality Model Development

The modeled SGD and associated nutrient loads from each SGD plume (referred to as pourpoints, Figure 1) were diffused into the marine environment using a previously developed MWQ model (Delevaux et al., 2018; Wada et al., 2021). The water quality model implements a non-linear decay function up to 1.2 km offshore (Knee et al., 2010) and incorporates the impedance of moving planimetrically through water with a composite of two marine drivers known to affect diffusion (depth (m) and wave power (KW/m)) (Fabricius, 2005; Yu et al., 2003) (see Equation 2). The offshore threshold was based on aerial thermal infrared imagery measurement (Johnson et al., 2008) representing the offshore extent of the cold groundwater plumes from the study site and consultation with local experts.

$$N_i = n \times e^{(-c^2/D_c)} \quad (2)$$

where N_i = Grid cell value for diffused submarine groundwater discharge (m³/week) and nutrients flux (kg/week) per pourpoint i , n = Submarine groundwater discharge volume (m³/week) and nutrient load (kg/week) at each pourpoint (obtained from the GW model), c = diffusion factor layer value at each grid cell (unitless), and D_c = distance threshold from the shore for each pourpoint (set to 1.2 km).

Then, all the individual groundwater and nutrient plumes from each pourpoint were summed to obtain the aggregated SGD and nutrient plume at the study site scale, per management scenario. It should also be noted that the locations of MWQ results are predetermined based on the simulated SGD plumes. Therefore, the lack of results along some sections of the coastline does not mean that nutrients are unable to enter the ocean in these areas. This model poses several limitations. It is a diffusive approach that accounts for wrapping around coastal features, but does not capture the nearshore advection forces that push SGD or nutrients in specific directions (Halpern et al., 2008). The model was applied at the weekly scale to align with the length of the lab experiments (further discussed in Section 2.6.1). To link the MWQ model to the algae experiment, we divided the weekly nutrient loads (kg/week) converted to grams per week by the weekly SGD (m³) to obtain the nutrient concentrations (g/m³) of water discharging into the marine environment.

2.6. Algae Predictive Modeling

2.6.1. Manipulative Experiments

To adequately predict the effects of environmental change at a fine-scale local ecosystem level, it was important to first define important relationships between the ecosystem and the physiological traits of the organisms that thrive within its parameters. Through manipulative experiments on two relevant algal species (*H. musciformis* and *U. lactuca*), the physiological attributes of these organisms are described and compared in the context of an SGD gradient from oceanic to groundwater seep conditions, and the predicted outcomes of these two species are assessed within the framework of known climate change threats.

Eight iterations of the experiment were conducted from September–November 2021. Each iteration ran as follows: Six individual plants of *H. musciformis* and *U. lactuca* were collected during a negative low tide at Wawamalu, O'ahu, and were immediately transported in seawater to the Marine Macrophyte Lab greenhouse at the University of Hawai'i at Mānoa. All plants were kept in approximately 2 L of unfiltered seawater in 10 L aquaria for 8 days in a partially shaded outdoor area to acclimate and draw down internal nutrient supplies following Dailer et al. (2012). Tanks were aerated, covered with clear plastic lids, and periodically checked for salinity changes; seawater was not changed during the drawdown phase. The day before the start of the experiment, algae were sectioned into four replicate pieces, each 0.28–0.3 g in wet weight using a Sartorius TE214S digital analytical balance (precision to 0.0001 g; Sartorius AG, Göttingen, Germany), and returned to the aquaria.

The experiment commenced the following morning at 08:00 with photographs, rapid light curves (RLCs) measuring photosynthetic efficiency, and wet weighing of each individual (24 per species). Randomly chosen replicates were patted dry with paper towel three times and weighed with the Sartorius TE214S balance then placed

Table 2
Salinity and Nutrient Concentrations for Experimental Algal Treatments

Water quality parameter	0	1	2	2.5	3	4
Salinity (‰)	35	35	28	28	18	11
Nitrate (μmol)	0.5	14.3	27.1	52.9	52.9	80.0
Phosphate (μmol)	0.005	0.005	0.15	1.64	1.64	3.79

Note. All treatments were run at ~20, 27, and 30°C.

in individual jars with 700 mL of seawater at the correct dilution for each treatment. Treatments consisted of paired salinity and nutrient concentrations to simulate a gradient from coastal ocean to coastal spring conditions with decreasing salinity ranging from 35 to 11 ppt and increasing nitrate ranging from 14 to 80 μmol (Table 2). These values (as well as phosphate and temperature) follow Johnson et al. (2008) results from naturally occurring Kona SGD inputs. Seawater was pre-filtered with a 0.22 μm Millex Stericup® filtration system (Millex Sigma, Darmstadt, Germany), diluted with deionized water to achieve the various salinities, and stored in 20 L carboys. After all replicates were placed in jars, each received the appropriate inoculation of nitrate and phosphate (Table 2) and were equipped with air tubes that gently agitated and aerated the water. For simplicity in the text, we refer to these combined nitrate/phosphate inoculations as “nitrate” (N). Eight jars were nested in clear, plastic, water-filled bins, and were raised on plastic egg crates above 500-W titanium aquarium heaters (Finnex TH-05005; Illinois, USA). Three daytime temperatures (~20, 27, 30°C) were maintained within the bins from 06:00 to 18:30 every day during the experiment. Evening and nighttime temperatures dropped to ambient (~17–20°C) in the air-conditioned greenhouse. Bins were arranged side-by-side under a PVC pipe structure covered in one layer of light-colored shade-cloth that reduced ambient irradiance by ~50% with minimal obstruction. Water changes and fresh inoculations were done every 2 days and to avoid bin effects, each set of jars was moved counterclockwise to the adjacent bin and their positions within the bins were shifted from front to back. Bin temperatures were adjusted accordingly. Wet weight was subsequently measured on the fifth and ninth days, which concluded the experimental run and yielded a total of two replicates per treatment/temperature combination. The entire process was repeated seven times with a final total of 16 replicates.

Wet weight was recorded and growth rate percent was calculated using the equation:

$$((w_f - w_i)/w_i) \times 100 \quad (3)$$

where f = final and i = initial wet weight (w). This equation is commonly used (Dailer et al., 2010) and eliminates the need for assumptions of steady or exponential growth because these parameters have not been well documented in *U. lactuca* or *H. musciformis* (Lobban and Harrison, 1994).

Growth data were analyzed by species using linear mixed-effects model packages lme4 and lmerTest in R Statistical Software (v2021.09.0 R Core Team). Graphs were plotted using the ggplot2 package (v3.3.6, Wickham, 2016). The model formula specified treatment and temperature as fixed effects and run (to account for irradiance changes over time), RLC order (final processing order), lunar phase (affecting *U. lactuca* only), and plant ID (inherent plant variability) as random effects. The best model fit for *U. lactuca* included plant ID, lunar phase, and run as random effects whereas plant ID, run, and RLC order provided the best fit for *H. musciformis* (Barr et al., 2013), and in each case avoided issues of singularity. Bartlett's test was used to check for equal variance, and Welch's Analysis of Variance (ANOVA) was used for significance testing. Subsequently, ad hoc pairwise comparisons using the Games Howell test were run (where appropriate) to identify significant differences between the treatments.

After identifying important knowledge gaps in the dataset, the experiment was repeated but focused on two new treatments (Treatment 0: 35 ppt/0.5 μmol N and Treatment 2.5: 28 ppt/53 μmol N) at the three temperatures. For this iteration, 48 plants of each species were collected, acclimated, and one 0.28–0.30 g piece per plant was placed in 700 mL of seawater to commence the experiment as described above. Data were added to and analyzed with the original dataset. Several *U. lactuca* replicates in treatment 2.5 (Table 2) experienced significant tissue sloughing, likely due to reproduction, and thus this treatment was omitted from the analysis.

2.6.2. Macroalgal Spatial Predictive Modeling—Calibration

Boosted regression trees were calibrated to derive the relationship between change in algae weight and environmental drivers in these SGD simulations (salinity, temperature, N and P, Table 2) (Elith & Leathwick, 2013). Two separate models were calibrated, one for *U. lactuca* and one for *H. musciformis*, to determine the most influential SGD associated drivers (among the simultaneously tested drivers) and characterize the relationships between the modeled algae and the SGD drivers using response curves. The change in biomass of *U. lactuca* and

H. musciformis measured during the manipulative experiments were used as the response variables and a square root transformation was applied to improve the normality of the response variable distributions. The boosted regression trees were run using a Gaussian (normal) distribution given the continuous nature of the response variables. The calibration (training) and cross-validation (CV) percent deviance explained (PDE) were used as metrics of model performance (*U. lactuca* Training PDE: 21.2% and CV PDE: 18.5%; *H. musciformis* Training PDE: 23.2% and CV PDE: 15.0%). The two predictive models were used to predict the spatial change in habitat suitability of *U. lactuca* and *H. musciformis* across the study area following the development of the groundwater and MWQ models.

2.6.3. Macroalgal Spatial Predictive Modeling—Scenario Application

The two calibrated predictive models were applied to spatially extrapolate the change in habitat suitability of *U. lactuca* and *H. musciformis* across the study area by using the modeled SGD drivers under current conditions and each future scenario. These geospatial predictors (60 m \times 60 m) were the outputs of the groundwater and MWQ models. Salinity and temperature were derived from the groundwater model and the nitrogen and phosphorus concentrations were derived from the MWQ models. The current distribution of both algal species were mapped using the predictive models and the field data for *U. lactuca* was used to validate the *U. lactuca* model. The *H. musciformis* model could not be ground-truthed because it is not currently present within the study area. After mapping the predicted biomass of both species under each scenario, the area (ha) where *U. lactuca* biomass is likely to increase or decrease, and the area where *H. musciformis* biomass could increase if introduced to Hawai'i Island, were computed.

2.6.4. Macroalgal Spatial Predictive Modeling—Field Validation

To validate the predicted habitat suitability of *U. lactuca*, the percent cover of *U. lactuca* was quantified in the field using a quadrat-based point-intercept method (Figure 2g). Based on the known locations of major SGD plumes (Johnson et al., 2008) simulated in the models, seven SGD-influenced sites and two non-SGD sites were selected for 10-m transect surveys to analyze benthic cover along the Keauhou coastline. To establish the transect surveys, GPS start points were generated at four distance strata from known SGD plume locations (for SGD-influenced sites: 0–20 m, 20–50 m, 50–200 m, and 200–500 m) and three stratified depths (intertidal, 0–2 m, and 2–5 m). If *U. lactuca* was present, adjacent start points were moved within the appropriate depth and distance strata to include the *U. lactuca* patch and a new GPS point was recorded. Five to 10 transects were surveyed per site depending on logistics and site conditions. At the 2–5 m strata, presence of *U. lactuca* was not expected, thus photo surveys were instead conducted to note the absence of *U. lactuca* and the characteristics of the surrounding environment. Benthic cover data was gathered within 0.25 m² quadrats placed at 1 m intervals on alternating sides of the transect tape, with 16 classification points per quadrat (Stamoulis et al., 2017). As predicted, *H. musciformis* was not observed in the field. Additional information regarding field methods are provided in Supporting Information S1—Section 3. To validate the *U. lactuca* model, the predicted change in habitat suitability values at each survey site were extracted, and the modeled values were compared to the observed percent cover using a linear regression analysis (with *p*-values).

3. Results and Discussion

3.1. Baseline Land-Sea Modeling

3.1.1. Algae Manipulative Experiment Results for Simulated SGD

Ulva lactuca growth increased with increasing proximity to simulated SGD pourpoint conditions. The highest mean 8-day growth rate (50.0%) occurred in the treatment with the largest increase in nutrients (80 μ mol N) paired with the largest decrease in salinity (11 ppt), regardless of temperature (Figure 3a). Significant differences in *U. lactuca* growth rates were found, in particular, between the oligotrophic 35 ppt/0.5 μ mol N treatment and all other treatments ($p < 0.01$) and between the 35 ppt/14 μ mol N and 11 ppt/80 μ mol N treatments ($p = 0.02$). Temperature did not have a significant effect on growth ($p = 0.85$). Further details of the statistical analysis can be found in Supporting Information S1—Section 4.

In general, *H. musciformis* growth decreased with proximity to simulated SGD pourpoint conditions, although the relationship was more complex. Two treatments had virtually the same 8-day mean growth rates and were the highest among all treatments (35 ppt/14 μ mol N [35.3%] and 28 ppt/53 μ mol N [34.6%]; Figure 3b). We determined that salinity was a major factor in *H. musciformis* growth when we paired 28 ppt salinity (as in treatment 2) with 53 μ mol N (as in treatment 3). The mean growth rate for this new treatment (treatment 2.5; 34.6%) was

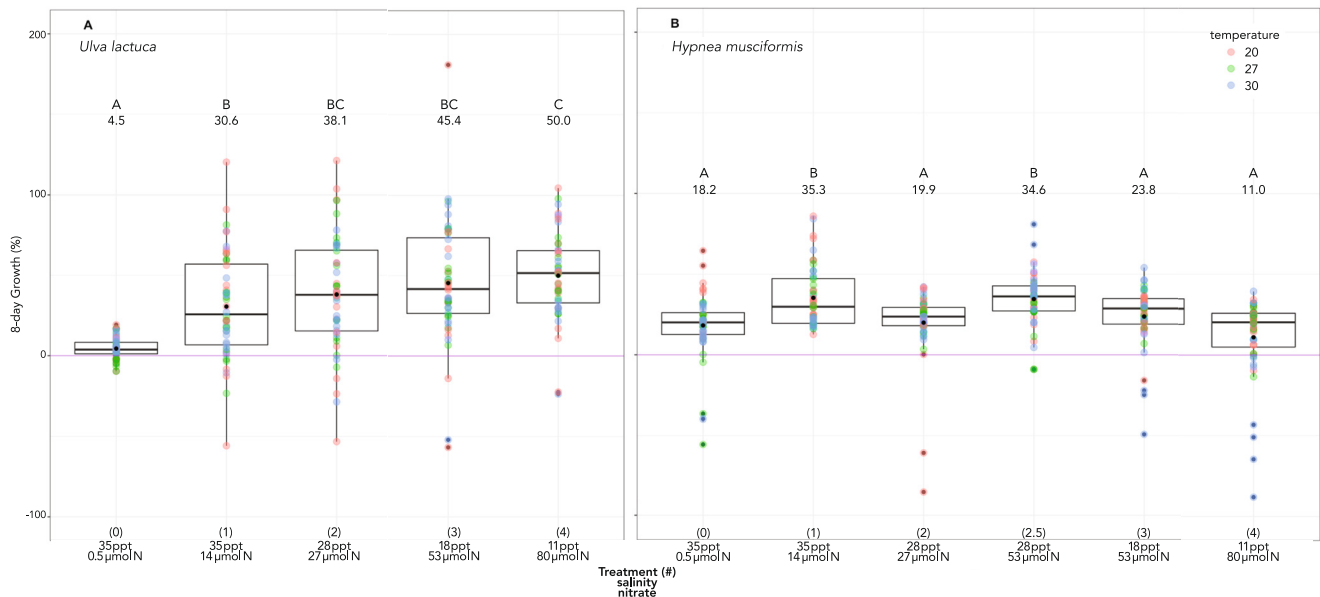


Figure 3. Boxplot of 8-day growth rate by treatment for (a) *Ulva lactuca* and (b) *Hypnea musciformis*. Mean of salinity/nutrient treatments indicated by black dots. Significance results of pairwise comparisons denoted (a, b, c) with reported mean value above individual boxes. X-axis labels represent salinity in parts per thousand (ppt) and amount of nitrate in μmol . Colored data points represent temperature and the purple horizontal line indicates zero growth.

statistically higher than that of both treatments 2 ($p = 0.05$; 19.9%) and 3 ($p = 0.005$; 23.8%). When salinity decreased to 18 ppt and below, the mean growth rate of *H. musciformis* decreased, even with an increase in nutrients (Figure 3b). As with *U. lactuca*, the effect of temperature on the growth rate of *H. musciformis* was not significant ($p = 0.27$). Additional studies are underway to clarify the non-linear relationship with nutrients-SGD conditions to aid model interpretation.

3.1.2. Influences of SGD Quality on *Ulva lactuca* and *Hypnea musciformis* Growth

Ulva lactuca and *H. musciformis* had similar mean 8-day growth rates—30.6% and 35.3%, respectively—in full oceanic salinity (35 ppt) with modestly elevated nutrients (14 μmol N). *Ulva lactuca*, however, demonstrated higher growth rates in conditions similar to groundwater seeps (treatment 4). After 8 days, the mean biomass increase in *U. lactuca* was 50.0%. This suggests that this native species is adapted to thrive along Hawai'i's coastlines where abundant SGD springs decrease coastal salinity and increase nutrient concentrations.

In contrast, growth rates of *H. musciformis* declined with decreasing salinity despite increasing nutrient concentrations. With a moderate salinity decrease from 35 to 28 ppt and a near double increase in nitrate (14–27 μmol N), *H. musciformis* mean growth significantly declined from 35.3% to 19.9% ($p < 0.001$). The nitrate concentration needed to bring the 28 ppt growth rate back in range with the 35 ppt growth rate, was more than three times greater (from 14 to 53 μmol N). These results suggest that SGD-dominated conditions are unsuitable for this invasive species but also indicate that it would grow adequately in Kona if coastal salinities were to increase to 28 ppt, assuming the nutrient inputs also remained adequately high. Based on these data, the likely mean growth rate for *U. lactuca* at 28 ppt/53 μmol N would be between 38.1% and 45.4% and would still be higher than that of *H. musciformis* (34.6%). This is important because conditions reverse, in favor of *H. musciformis*, as salinity increases above 28 ppt, and these conditions are likely to occur off the coast where SGD waters mix with ocean water. Similar patterns were observed in regions of Maui where *H. musciformis* grew in bloom conditions off the coast, impacting the nearshore zones (Dailer et al., 2010). Our results are a clear indication that algal physiological characteristics are important factors in determining species-specific distributions in SGD-influenced ecosystems and highlight native species vulnerability to changes in ecosystem parameters.

3.1.3. *Ulva lactuca* and *Hypnea musciformis* Model Calibration

The *U. lactuca* and *H. musciformis* regression models, which describe the relationship between the environmental drivers and change in algae weight, were calibrated using data from the manipulative experiments. *Ulva lactuca* demonstrated a positive, linear growth rate with decreasing salinity and increasing N concentrations (Figure 4a).

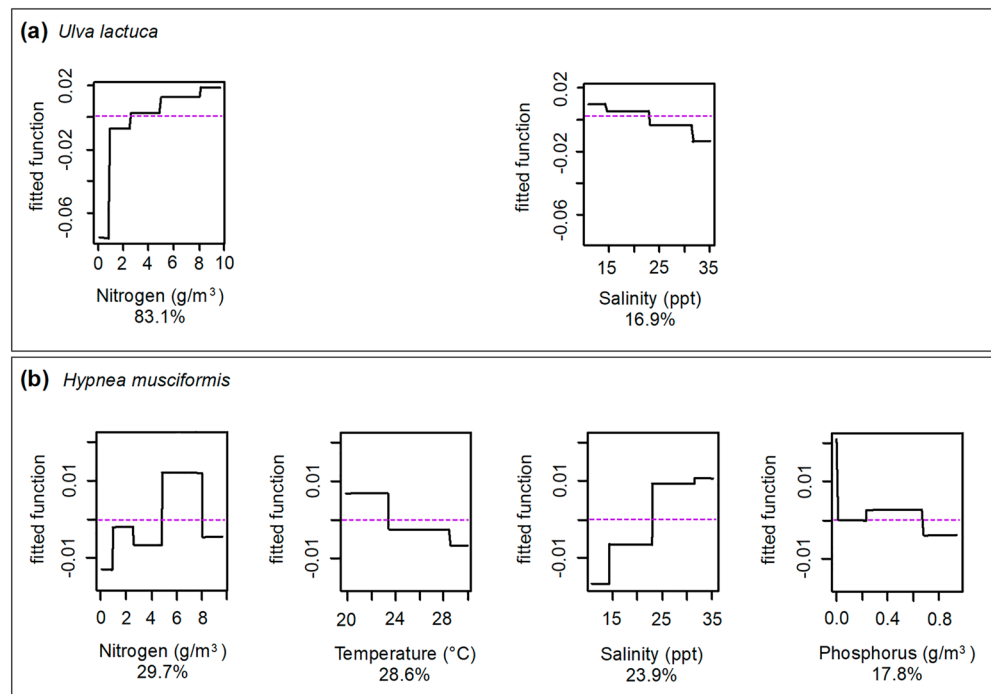


Figure 4. Regression modeling response curves for (a) *Ulva lactuca* and (b) *Hypnea musciformis* with respect to the modeled parameters: salinity, temperature, nitrogen, phosphorus. Temperature and phosphorus curves are not shown for *U. lactuca* because those two parameters were not important predictors of the *U. lactuca* model. Percentages represent the relative predictive importance of each parameter. Dashed purple horizontal line indicates zero growth.

Results from the regression model suggest that temperature and P are not important predictors for *U. lactuca*. For *H. musciformis*, a dip in the fitted function between 3–5 and 8–10 g/m³ N was observed (Figure 4b). The dip was due to the fact that *H. musciformis* requires higher salinities to maintain a positive growth rate, but the experimental treatments followed a gradient that paired high N with salinity concentrations too low to maintain a positive growth rate. It is also noted that *H. musciformis* growth was positively associated with increasing salinity. These salinity-nutrient findings suggest that *H. musciformis* will not grow near freshwater sources but could leverage high nutrient conditions within a narrow, moderately-high salinity range.

3.1.4. Baseline Groundwater, Marine Water Quality, and Spatial Predictive Model Results

Due to the non-linear relationship between the hydrologic parameters (hydraulic head, salinity, N, P) exhibited in the Keauhou coastal aquifer, accurate calibration results are difficult to obtain (Okuhata et al., 2021). Nonetheless, the hydraulic head is well calibrated under density-dependent conditions, with an RMSE of 0.39 m. At simulated SGD pourpoints, salinity concentrations range from 12 to 27 ppt (Figure 5a) and N concentrations range from 0.5 to 7.0 mg/L (Figure 5b). Significantly higher concentrations are simulated within the Keauhou aquifer system downstream of point-source pollution locations, such as cesspools and the Kealakehe WWTP.

The spatial predictive model, which uses water quantity and quality results from the groundwater and MWQ models as inputs, estimates that *U. lactuca* biomass ranges from 0.02 to 0.13 g (Figure 5c). This is compared to field measurements of *U. lactuca* percent cover, which range from 0% to 26% (Figure 5c). A statistically significant relationship ($p < 0.001$) was found between the observed *U. lactuca* cover from field surveys and the predicted biomass produced from the predictive model (Figure 5d). Therefore, the baseline model (Scenario 0) served as a reliable tool to assess the spatial change in *U. lactuca* biomass and to test scenario applications. As previously mentioned, because *H. musciformis* is currently not found along the Kona coastline, it could not be validated in the field.

3.2. Climate and Land Use Influences on Groundwater and Marine Water Quality

Changes in groundwater and MWQ vary across the Keauhou basal aquifer and across all scenarios (Table 3). Because temperature and P were not considered to be important predictors of the *U. lactuca* regression model, SGD quantity, salinity, and N will be the primary predictors discussed here.

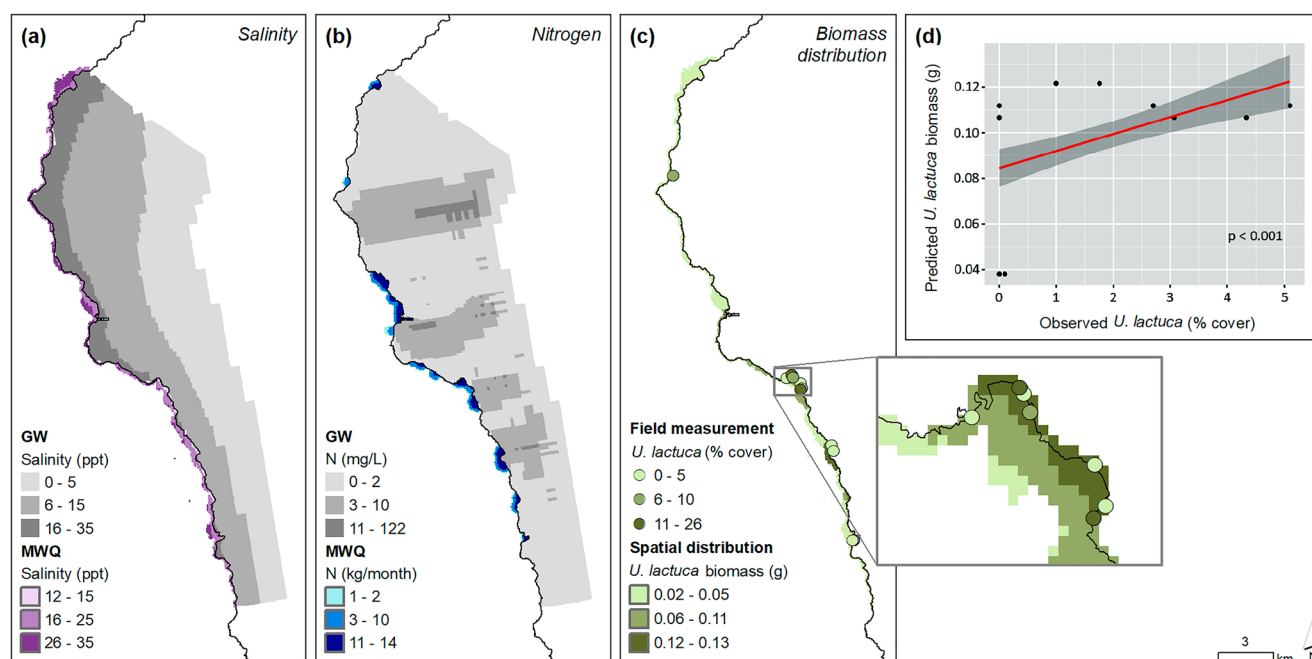


Figure 5. Baseline groundwater and marine water quality results. (a) Salinity calibration; (b) Nitrogen calibration; (c) Baseline spatial distribution of *U. lactuca* biomass and *U. lactuca* field measurements; (d) Validation plot between observed and predicted *U. lactuca*. The plotted observed *U. lactuca* is transformed using the square root of the field measurements shown in panel (c).

3.2.1. Scenario 1: Climate Change

Future climate models following RCP 8.5 mid-century project lower rainfall (Elison Timm et al., 2015) and thus reduce groundwater recharge over the Keauhou aquifer by 37%. Therefore, under the assumptions of *Scenario 1: Climate Change*, hydraulic head will decline and the smaller hydraulic gradient will ultimately result in a loss of SGD quantity. Specifically, SGD quantity is projected to decline by $-255,000 \text{ m}^3/\text{month}$ (Figure 6a) in comparison to baseline results. With less SGD exiting, saltwater may flow into the aquifer, which increases the average salinity by 2.5 ppt within the SGD plumes. Additionally, N concentrations are projected to increase slightly within the aquifer because nutrients sourced from existing urban development and wastewater infrastructure will not be as readily diluted. The marine quality model shows a clear correlation between an increase in groundwater nitrogen concentrations and an increase in nitrogen mass loading in the marine water (Figure 6a), which demonstrates that terrestrial nutrient sources travel downgradient toward the coastline. Overall, groundwater and marine water temperatures are not projected to be significantly affected by climate change induced reductions in precipitation, where the simulated change in temperature remains within 1°C (Figure 6a). Finally, growth experiments

Table 3
Change in Total SGD Quantity, Average Salinity, and Total Nitrogen Flux at SGD Plumes, and Predicted Macroalgae Biomass Distribution for Each Scenario

Scenario	Change in groundwater parameter			Change in macroalgae predicted biomass distribution			
	SGD quantity (m^3/mo)	Average salinity (ppt)	Nitrogen (kg/mo)	Increase habitat suitability of <i>U. lactuca</i> (ha)	Decrease habitat suitability of <i>U. lactuca</i> (ha)	Increase habitat suitability of <i>H. musciformis</i> (ha)	Decrease habitat suitability of <i>H. musciformis</i> (ha)
Impacts of climate change (relative to baseline results)							
Climate change	$-255,000$	$+2.5$	$+120$	$+60$	-198	$+219$	-66
Impacts of land use change (relative to climate change results)							
Urban development	$-162,000$	$+1.6$	$+5,000$	$+112$	-106	$+209$	-59
Native forest conversion + Urban development	$-255,000$	$+2.6$	$+5,700$	$+96$	-192	$+260$	-74

Note. The Climate Change scenario results are relative to baseline model results. The Urban Development and Native Forest Conversion scenario results are relative to Climate Change scenario results. Positive values indicate an increase and negative values indicate a decrease.

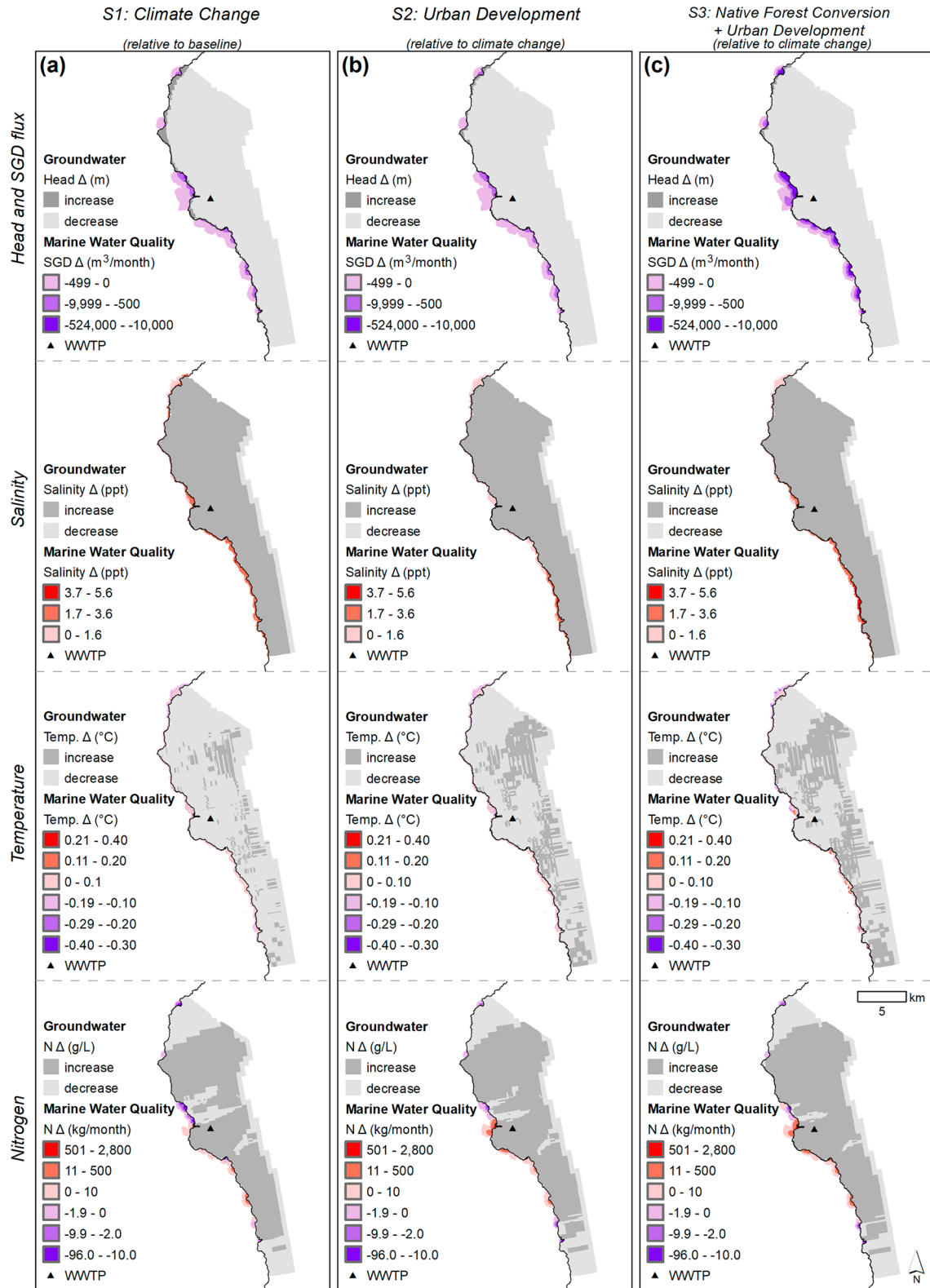


Figure 6. Scenario groundwater and marine water quality results. (a) Climate Change, (b) Urban Development, and (c) Native Forest Conversion + Urban Development scenario effects on SGD, salinity, temperature, and nitrogen.

demonstrate that both algae had wide ranges of temperature tolerance (Figures 3a and 3b) and suggest that temperature would not emerge as a major factor modifying growth in this scenario.

3.2.2. Scenario 2: Urban Development

Under the assumptions of *Scenario 2: Urban Development*, native forests are protected from the invasion of higher-water-use plant species, which mitigates an additional loss of recharge that would occur without such protection (Bremer et al., 2021). Compared to climate change only conditions, this scenario predicts a loss of $-162,000 \text{ m}^3/\text{month}$ of SGD quantity due to recharge reductions from combined climate change and urban development effects (Figure 6b). Therefore, the difference in SGD quantity results between Scenarios 1 and 2 (Table 3) is due to the influence of urban development. Both scenarios assume future climate conditions and native forest protection, but Scenario 2 also assumes that Keauhou will be further developed according to granted development permits (Fukunaga & Associates, Inc., 2017;). With this development, it is predicted that water demands will increase by $64,080 \text{ m}^3/\text{d}$ (Fukunaga & Associates, Inc., 2017), and this study assumes that the additional water demand will be extracted from the pumping wells in the high-level aquifer area. Because of the additional groundwater that would be withdrawn from the high-level aquifer area, there is a decrease in groundwater flux entering the basal Keauhou aquifer, which results in increased salinity and less nutrient dilution. Furthermore, this study assumes that 50% of the additional water demand will be routed to the Kealakehe WWTP as wastewater effluent (Board of Water Supply, 2021; Okuhata et al., 2021). The additional groundwater extraction and wastewater effluent result in a significant increase in nitrogen concentrations projected along the coastline. Under this scenario, nitrogen mass loads will increase by $5,000 \text{ kg/month}$ relative to climate change conditions, which is almost 42 times greater than the nitrogen loads predicted with climate change only (Table 3).

3.2.3. Scenario 3: Native Forest Conversion + Urban Development

If native forests are not protected, permitted land is developed, and climate change assumptions persist, recharge is projected to be reduced by 45% (in comparison to 37% reduction under only climate change). Therefore, under the assumptions for *Scenario 3: Native Forest Conversion + Urban Development*, SGD quantity is projected to decrease by $-255,000 \text{ m}^3/\text{month}$ relative to only climate change conditions (Figure 6c) because of a decrease in groundwater recharge caused by climate change, increased groundwater extraction to meet higher water demands, and increased evapotranspiration rates as a result of invasion by higher-water-use forest species. The effects of forest protection are most evident between Scenarios 2 and 3, where the only modeled difference is the protection of native forests. Therefore, if high-water-use species are allowed to invade native forests, SGD quantity will be further reduced by $93,000 \text{ m}^3/\text{month}$ (Table 3). Due to this change in freshwater flux, the average salinity is projected to increase by 2.6 ppt and N loads by $5,700 \text{ kg/month}$, which are both higher than the native forest protection scenario despite both scenarios including additional urban development.

3.3. Predicted Habitat Suitability Change

3.3.1. *Ulva lactuca* Habitat Suitability Change

Compared to the baseline scenario, *U. lactuca* habitat suitability under *Scenario 1: Climate Change* diminishes along 198 ha (Table 3; Figure 7a). The reduced recharge caused by climate change effects is a dominating factor that negatively impacts the habitat suitability of *U. lactuca* by increasing salinity. Habitat suitability, however, will also expand along 60 ha, primarily in areas where nitrogen is expected to increase, thus counteracting influences of salinity. The remaining scenarios both assume a dry future climate, so changes in habitat suitability are compared to *Scenario 1: Climate Change* rather than baseline results. Thus, under *Scenario 3: Native Forest Conversion + Urban Development* assumptions, where both urban development ensues and native forests are not protected, *U. lactuca* habitat suitability diminishes along a larger area of 192 ha (Figure 7c). Under these scenario assumptions, SGD flux will decrease because of increased groundwater withdrawal and reduced recharge caused by climate change and higher-water-use forests and grasses, which ultimately does not favor *U. lactuca* growth. Under these same assumptions, however, habitat suitability will expand by 96 ha due to increased N loads associated with future urban development (particularly around the WWTP). In contrast, under *Scenario 2: Urban Development* assumption, where native forests remain protected, habitat suitability of *U. lactuca* only diminishes along 106 ha while expanding along 112 ha (Figure 7b). This is likely due to the combination of adverse salinity increases caused by reduced SGD and beneficial nitrogen increases as a result of urban development. These two opposing effects counterbalance spatial distribution changes and this relationship emphasizes the importance of simultaneously evaluating all water quantity and quality parameters that may influence coastal ecosystem health.

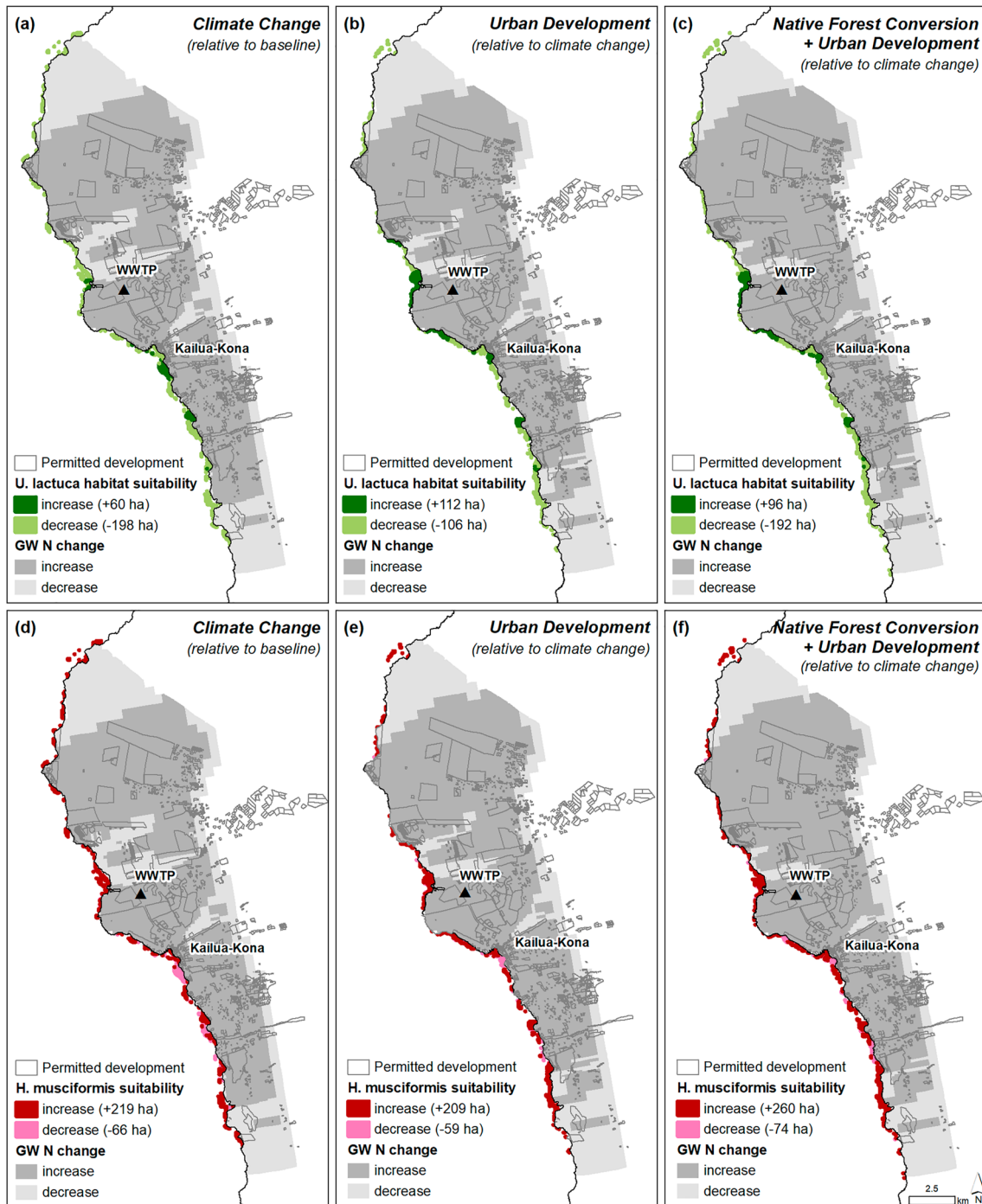


Figure 7. Compiled predicted habitat suitability change of (a)–(c) *U. lactuca* biomass and (d)–(f) *H. musciformis* occurrence for each scenario. Results in panels (a) and (d) are relative to baseline scenario results. Results in panels (b), (c), (e), (f) are relative to climate change scenario results.

In all three scenarios, the expansion of *U. lactuca* habitat suitability primarily increased in areas with the most significant elevation of nutrient levels. These areas include the Honokohau Harbor, which is downgradient of the Kealakehe WWTP, and near the densely-populated town of Kailua-Kona (Figure 7). Kailua-Kona is expected to be further developed and the model assumes that wastewater effluent produced from the increased development will be directed to the Kealakehe WWTP, which will introduce additional nutrients to the localized areas. Therefore, the coastlines adjacent to those specific areas will discharge a higher nitrogen flux, which will result in increased *U. lactuca* growth. While these scenarios suggest overall positive outcomes for *U. lactuca*, the growth

experiments did not address growth rates in higher nitrogen conditions, especially at full salinities. Further, the growth experiments targeted *U. lactuca* in isolation, thus not accounting for interactions in the coastal ecosystem (i.e., grazing by urchins and other herbivores).

3.3.2. *Hypnea musciformis* Habitat Suitability Change

In contrast to *U. lactuca*, all three scenarios increase habitat suitability for *H. musciformis*. In all scenarios, there is a reduction in SGD discharge due to climate change, additional pumping, decreased recharge, or a combination of the three. This decline in freshwater results in an increase in salinity, and because *H. musciformis* prefers salty water, a decline in freshwater availability promotes growth. Under the *Scenario 1: Climate Change*, 219 ha of the coastline will promote the occurrence of *H. musciformis*, while only 66 ha of the coastline would be considered unsuitable (Table 3; Figure 7d) compared to baseline scenario results. Relative to climate change only conditions, 209 ha of the coastline will be suitable for *H. musciformis* growth while 59 ha will be unsuitable under *Scenario 2: Urban Development* (Figure 7e). Comparatively, and also relative to climate change only conditions, *Scenario 3: Native Forest Conversion + Urban Development* designates 260 ha of habitable coastline and 74 ha of inhabitable coastline (Figure 7f).

Increased salinity simulated at the pourpoints will drive conditions back into tolerance for *H. musciformis* (Figure 3b), therefore promoting growth of this invasive species. *Hypnea musciformis* growth along this SGD-nutrient gradient, however, is non-linear, thus making growth estimates difficult to predict in the absence of growth data. Expanded physiological studies in the upcoming manuscript (Richards Donà et al., in prep) aim to clarify patterns.

4. Conclusions

Populations of diverse marine algae reflect evolving SGD conditions, which are typically representative of various land and water management practices applied at watershed levels. Thus, these marine algae serve as important indicators of nearshore GDE health in the context of multiple drivers of environmental change (Dulai et al., 2021). In Hawai'i, particularly within the Keauhou aquifer, there is increasing attention to the importance of understanding the impacts of intersecting climate, land, and water management changes on GDEs due to their important role as public trust resources (Adler & Ranney, 2018). Yet despite the interest in protecting GDEs, there has been little quantitative work to understand the potential impacts of such drivers on GDEs and indicator species, such as macroalgae (Dulai et al., 2021). Accordingly, this study combined lab and field work with an adapted ridge-to-reef modeling framework (Delevaux et al., 2018; Okuhata et al., 2021) to examine how a dry future climate, urban development, and native forest conversion may influence SGD conditions and the growth of the native and culturally valuable *U. lactuca* and the potentially invasive *H. musciformis* across the Keauhou aquifer. In-so-doing, this study offers a new approach that integrates manipulative lab experiments with modeling tools and field data to identify land-sea management solutions that address future impacts of land use and climate change on GDEs in tropical environments.

While few other algal species have been examined for SGD influence, one pair of congeneric native and invasive species (*Gracilaria coronopifolia* and *Gracilaria salicornia*) have been characterized by growth experiments under a range of set SGD conditions (Amato et al., 2018; Dulai et al., 2021). Findings from this study add two new species and suggest that *U. lactuca*'s growth was highest in low-salinity and moderate- to high-nutrient conditions, which supports the view that many native algae are adapted to SGD habitats (Amato et al., 2018; Duarte et al., 2010; Huisman et al., 2007). Although *U. lactuca* is a native species, blooms of this species are not necessarily a positive outcome if fed by wastewater nutrients. Additionally, because most of the modeled nitrogen originates from wastewater (Okuhata et al., 2021), it is likely accompanied by other wastewater components (i.e., organic pollutants, heavy metals) that may have negative effects on GDEs.

In contrast, growth rates of *H. musciformis* were not linear, but generally declined with reduced salinity despite increasing nutrient concentrations. This outcome suggests that *H. musciformis* is not well-adapted to natural SGD conditions observed in Keauhou, where nutrients are transported to the coastline via underground conduits. *Hypnea musciformis*, however, may become an increasing threat with reduced SGD flow coupled with increases in nutrients. With so few experimental studies, it is expected that a range of responses will be seen across the diversity of native algae. Nonetheless, this study establishes an overall new framework for lab experiments that can test a range of physiological performances in needed efforts to estimate the physiological ecology of invasive

algae as native habitat ranges of salinity and nutrients are altered to new, non-native ranges. The finding of non-native intolerance to native habitat abiotic parameters establishes new urgency for testing other invasive species to establish if those invasives possess hidden characteristics that make them intolerant to native habitats (an “Achilles’ heel”).

Further, the modeled scenarios suggest that a dry future climate (RCP 8.5 mid-century), increased urban development, and conversion of native forest to non-native species reduce SGD flux to the coastline, which could have overall negative effects on *U. lactuca*. In contrast, these changes appear to favor growth of *H. musciformis* if it were to become established across Keauhou’s coastline. Although *H. musciformis* is currently not documented to exist in Kona, this invasive species may easily spread from the Island of Maui once coastal water conditions are driven toward *H. musciformis*-favored conditions. Although a dry climate and increased development are predicted to have significant negative impacts on SGD quantity, the preservation of native forests appears to serve as an effective management strategy to mitigate SGD loss. Actionable steps can therefore be adopted to lessen the loss of SGD when considering tradeoffs between increased development and protecting native forests from invasion of higher-water-use invasive forest cover and grasslands in the face of climate change. Ecohydrological data on various forest types, however, is still relatively limited in Hawai’i and the tropics (Wright et al., 2017), and future research can help to refine these results.

Finally, this study demonstrates the benefits of using an integrative ridge-to-reef framework to better understand how the quantity and quality of groundwater and coastal waters, driven by watershed management, link to macroalgal growth under varying drivers of environmental change. By linking lab work, field work, and stacked models, this novel study demonstrates how *U. lactuca* thrives on the combination of nutrient-freshwater volumes, which is mediated by upstream watershed management. Further, this study identifies numerous fine-scale areas that appear vulnerable to the invasion of *H. musciformis* along the Kona coastline. The complex relationships identified throughout this work emphasize the importance of simultaneously evaluating the effect of land cover and climate change on multiple water quantity and quality parameters that may influence coastal ecosystem health as well as responses by algae to those parameters. This framework and approach can be adapted to investigate the land-sea effects on marine ecosystems of other coastal aquifers around the world.

Data Availability Statement

Datasets used for this research (model outputs and lab experiments) are available at <https://doi.org/10.5281/zenodo.8084889>. Additionally, datasets used for groundwater model calibration are available in the Supplementary Material of Okuhata et al. (2021) via <https://doi.org/10.1007/s10040-021-02407-y>.

Acknowledgments

We would like to acknowledge the West Hawai’i community for their continuous support. We thank the Queen Lili’uokalani Trust, Kamehameha Schools, and the Cesspool Working Group for their insight and guidance. Thank you to Nathan DeMaagd for assistance in developing the groundwater recharge scenarios and Gregory Chun for input and collaboration throughout the process. This paper is SOEST Contribution no. 11693, contributed paper CP-2024-01 from the Water Resources Research Center, and paper #200 from the School of Life Sciences, University of Hawai’i at Mānoa. Funding for this project came from the USGS Water Resources Research Institute Program Grant G16AP00049 BY5, the Hawai’i EPSCoR Program, funded by the National Science Foundation Research Infrastructure Improvement Award (RII) Track-1: ‘Ike Wai: Securing Hawai’i’s Water Future Award OIA-1557349, the Hawai’i Invasive Species Council PO C21591, and the National Fish and Wildlife Foundation Award 0810.20.068602.

References

- Abbott, I. A. (1978). The uses of seaweed as food in Hawaii. *Economic Botany*, 32(4), 409–412. <https://doi.org/10.1007/bf02907938>
- Abbott, I. A., & Shimazu, C. (1985). The geographic origin of the plants most commonly used for medicine by Hawaiians. *Journal of Ethnopharmacology*, 14(2–3), 213–222. [https://doi.org/10.1016/0378-8741\(85\)90089-3](https://doi.org/10.1016/0378-8741(85)90089-3)
- Abbott, I. A., & Williamson, E. (1974). *Limu, an ethnobotanical study of some edible Hawaiian seaweeds*. Pac. Trop. Bot. Gard.
- Adler, P. S., & Ranney, K. (2018). Adaptive management symposium on groundwater dependent ecosystems at Kaloko-Honokōhau National historical Park (KHNHP), meeting record and summary. Commission on water resource management, Kaloko-Honokōhau National historical Park Gateway center. Kailua Kona, Hawai’i. Retrieved from https://files.hawaii.gov/dlnr/cwrm/activity/keauhou/20181108-GDE_Symposium_Final.pdf. Accessed September 2022.
- Amato, D. W., Bishop, J. M., Glenn, C. R., Dulai, H., & Smith, C. M. (2016). Impact of submarine groundwater discharge on marine water quality and reef biota of Maui. *PLoS One*, 11(11), e0165825. <https://doi.org/10.1371/journal.pone.0165825>
- Amato, D. W., Smith, C. M., & Duarte, T. K. (2018). Submarine groundwater discharge differentially modifies photosynthesis, growth, and morphology for two contrasting species of *Gracilaria* (Rhodophyta). *Hydrology*, 5(4), 65. <https://doi.org/10.3390/hydrology5040065>
- Amato, D. W., Whittier, R. B., Dulai, H., & Smith, C. M. (2020). Algal bioassays detect modeled loading of wastewater-derived nitrogen in coastal waters of O’ahu, Hawai’i. *Marine Pollution Bulletin*, 150, 110668. <https://doi.org/10.1016/j.marpolbul.2019.110668>
- Analytical Laboratories of Hawai’i. (n.d.). Coral reef habitat maps of the main eight Hawaiian Islands from photointerpretation of aerial color photography, hyperspectral imagery and Ikonos satellite imagery. Report to NOAA. Retrieved from https://nccospublicstor.blob.core.windows.net/projects-attachments/208/Final%20Presentation%20by%20ALH_%20Hawaii_2007_Coral%20Reef%20Habitat%20Maps%20of%20the%20Main%20Eight%20Hawaiian%20Islands.pdf
- Babcock, R. W., McNair, D. A., Edling, L. A., & Nagato, H. (2004). Evaluation of a system for residential treatment and reuse of wastewater. *Journal of Environmental Engineering*, 130(7), 766–773. [https://doi.org/10.1061/\(asce\)0733-9372\(2004\)130:7\(766\)](https://doi.org/10.1061/(asce)0733-9372(2004)130:7(766))
- Barr, D. J., Levy, R., Scheepers, C., & Tily, H. J. (2013). Random effects structure for confirmatory hypothesis testing: Keep it maximal. *Journal of Memory and Language*, 68(3), 255–278. <https://doi.org/10.1016/j.jml.2012.11.001>
- Bell, P. R. F. (1992). Eutrophication and coral reefs: Some examples in the great barrier reef lagoon. *Water Research*, 26(5), 553–568. [https://doi.org/10.1016/0043-1354\(92\)90228-v](https://doi.org/10.1016/0043-1354(92)90228-v)

- Board of Water Supply. (2021). Xeriscape. Retrieved from <https://www.boardofwatersupply.com/conservation/xeriscape>. Accessed September 2021.
- Boulton, A. J. (2020). Conservation of groundwaters and their dependent ecosystems: Integrating molecular taxonomy, systematic reserve planning and cultural values. *Aquatic Conservation*, 30, 1–7. <https://doi.org/10.1002/aqc.3268>
- Bremer, L. L., DeMaagd, N., Wada, C. A., & Burnett, K. M. (2021). Priority watershed management areas for groundwater recharge and drinking water protection: A case study from Hawai'i island. *Journal of Environmental Management*, 286, 111622. <https://doi.org/10.1016/j.jenvman.2020.111622>
- Burnett, K. M., Elshall, A. S., Wada, C. A., Arik, A., El-Kadi, A., Voss, C. I., et al. (2020). Incorporating historical spring discharge protection into sustainable groundwater management: A case study from Pearl Harbor aquifer. *Hawai'i: Frontiers in Water*, 2, 542520. <https://doi.org/10.3389/frwa.2020.00014>
- Cantonati, M., Stevens, L. E., Segadelli, S., Springer, A. E., Goldscheider, N., Celico, F., et al. (2020). Ecohydrogeology: The interdisciplinary convergence needed to improve the study and stewardship of springs and other groundwater-dependent habitats, biota, and ecosystems. *Ecological Indicators*, 110, 105803. <https://doi.org/10.1016/j.ecolind.2019.105803>
- Conklin, E. J., & Smith, J. E. (2005). Abundance and spread of the invasive red algae, *Kappaphycus* spp., in Kane'ohe Bay, Hawai'i and an experimental assessment of management options. *Biological Invasions*, 7(6), 1029–1039. <https://doi.org/10.1007/s10530-004-3125-x>
- Dailer, M. L., Knox, R. S., Smith, J. E., Napier, M., & Smith, C. M. (2010). Using $\delta^{15}\text{N}$ values in algal tissue to map locations and potential sources of anthropogenic nutrient inputs on the island of Maui, Hawai'i, USA. *Marine Pollution Bulletin*, 60(5), 655–671. <https://doi.org/10.1016/j.marpolbul.2009.12.021>
- Dailer, M. L., Smith, J. E., & Smith, C. M. (2012). Responses of bloom forming and non-bloom forming macroalgae to nutrient enrichment in Hawai'i, USA. *Harmful Algae*, 17, 111–125. <https://doi.org/10.1016/j.hal.2012.03.008>
- Delevaux, J. M., Whittier, R., Stamoulis, K. A., Bremer, L. L., Jupiter, S., Friedlander, A. M., et al. (2018). A linked land-sea modeling framework to inform ridge-to-reef management in high oceanic islands. *PLoS One*, 13(3), e0193230. <https://doi.org/10.1371/journal.pone.0193230>
- Duarte, T. K., Pongkijvorasin, S., Roumasset, J., Amato, D., & Burnett, K. (2010). Optimal management of a Hawaiian Coastal aquifer with nearshore marine ecological interactions. *Water Resources Research*, 46(11), 11545. <https://doi.org/10.1029/2010WR009094>
- Dulai, H., Smith, C. M., Amato, D. W., Gibson, V., & Bremer, L. L. (2021). Risk to native marine macroalgae from land-use and climate change-related modifications to groundwater discharge in Hawai'i. *Limnology and Oceanography Letters*, 8(1), 141–153. <https://doi.org/10.1002/lol2.10232>
- Eamus, D., & Froend, R. (2006). Groundwater-dependent ecosystems: The where, what and why of GDEs. *Australian Journal of Botany*, 54(2), 91–96. <https://doi.org/10.1071/BT06029>
- Elison Timm, O., Giambelluca, T. W., & Diaz, H. F. (2015). Statistical downscaling of rainfall changes in Hawai'i based on the CMIP5 global model projections. *Journal of Geophysical Research: Atmospheres*, 120(1), 92–112. <https://doi.org/10.1002/2014JD022059>
- Elith, J., & Leathwick, J. (2013). Boosted regression trees for ecological modeling.
- Elshall, A. S., Arik, A. D., El-Kadi, A., Pierce, S., Ye, M., Burnett, K., et al. (2020). Groundwater sustainability: A review of the interactions between science and policy. *Environmental Research Letters*, 15(9), 093004. <https://doi.org/10.1088/1748-9326/ab8e8c>
- Engott, J. A. (2011). A water-budget model and assessment of groundwater recharge for the island of Hawaii. *US Geological Survey Science Investment Report*, 2011–5078. <https://doi.org/10.3133/sir20115078>
- Fabricius, K. E. (2005). Effects of terrestrial runoff on the ecology of corals and coral reefs: Review and synthesis. *Marine Pollution Bulletin*, 50(2), 125–146. <https://doi.org/10.1016/j.marpolbul.2004.11.028>
- Fackrell, J. K., Glenn, C. R., Thomas, D., Whittier, R., & Popp, B. N. (2020). Stable isotopes of precipitation and groundwater provide new insight into groundwater recharge and flow in a structurally complex hydrogeologic system: West Hawai'i, USA. *Hydrogeology Journal*, 28(4), 1191–1207. <https://doi.org/10.1007/s10040-020-02143-9>
- Fukunaga & Associates Inc. (2017). Hawai'i County water use and development plan update: Keauhou aquifer system. Retrieved from https://www.hawaiidws.org/wp-content/uploads/2018/06/Combined-Ph-1-2-Keauhou-20170510_w-Appendix-final.pdf. Accessed 8 October 2020.
- Giambelluca, T. W., Chen, Q., Frazier, A. G., Price, J. P., Chen, Y.-L., Chu, P.-S., et al. (2013). Online rainfall atlas of Hawaii. *Bulletin of the American Meteorological Society*, 94(3), 313–316. <https://doi.org/10.1175/BAMS-D-11-00228.1>
- Giambelluca, T. W., Shuai, X., Barnes, M. L., & Alliss, R. J. (2014). *Evapotranspiration of Hawai'i final report*.
- Gibson, V. L., Bremer, L. L., Burnett, K. M., Keaka Lui, N., & Smith, C. M. (2022). Biocultural values of groundwater dependent ecosystems in Kona, Hawai'i. *Ecology and Society*, 27(3), 18. <https://doi.org/10.5751/ES-13432-270318>
- Halpern, B. S., McLeod, K. L., Rosenberg, A. A., & Crowder, L. B. (2008). Managing for cumulative impacts in ecosystem-based management through ocean zoning. *Ocean & Coastal Management*, 51(3), 203–211. <https://doi.org/10.1016/j.ocecoaman.2007.08.002>
- Huisman, J. M., Abbott, I. A., & Smith, C. M. (2007). *Hawaiian reef plants*. University of Hawai'i Sea Grant College Program.
- Johnson, A. G., Glenn, C. R., Burnett, W. C., Peterson, R. N., & Lucey, P. G. (2008). Aerial infrared imaging reveals large nutrient-rich groundwater inputs to the ocean. *Geophysical Research Letters*, 35(15), L15606. <https://doi.org/10.1029/2008GL034574>
- Kløve, B., Ala-Aho, P., Bertrand, G., Gurdak, J. J., Kupfersberger, H., Kvernner, J., et al. (2014). Climate change impacts on groundwater and dependent ecosystems. *Journal of Hydrology*, 518, 250–266. <https://doi.org/10.1016/j.jhydrol.2013.06.037>
- Knee, K. L., Street, J. H., Grossman, E. E., Boehm, A. B., & Paytan, A. (2010). Nutrient inputs to the coastal ocean from submarine groundwater discharge in a groundwater-dominated system: Relation to land use. *Limnology & Oceanography*, 55(3), 1105–1122. <https://doi.org/10.4319/lo.2010.55.3.1105>
- Langevin, C. D., Thorne, D. T., Jr., Dausman, A. M., Sukop, M. C., & Guo, W. (2008). SEAWAT version 4: A computer program for simulation of multispecies solute and heat transport. *US Geological Survey Techniques and Methods Book*, 6, 39, chapter A22. <https://doi.org/10.3133/tm6a22>
- Lapointe, B. E. (1997). Nutrient thresholds for bottom-up control of macroalgae blooms on coral reefs in Jamaica and southeast Florida. *Limnology & Oceanography*, 42(5part2), 1119–1131. https://doi.org/10.4319/lo.1997.42.5_part_2.1119
- Lapointe, B. E., & O'Connell, J. D. (1989). Nutrient-enhanced growth of *Cladophora prolifera* in Harrington Sound, Bermuda: Eutrophication of a confined, phosphorus limited marine ecosystem. *Estuarine Coastal Shelf Science*, 28(4), 347–360. [https://doi.org/10.1016/0272-7714\(89\)90084-x](https://doi.org/10.1016/0272-7714(89)90084-x)
- Littler, M. M., Littler, D. S., & Brooks, B. L. (2006). Harmful algae on tropical coral reefs: Bottom-up eutrophication and top-down herbivory. *Harmful Algae*, 5, 565–585. <https://doi.org/10.1016/j.hal.2005.11.003>
- Lobban, C. S., & Harrison, P. J. (1994). *Seaweed ecology and physiology*. Cambridge University Press.
- Nakagawa, S., & Schielzeth, H. (2013). A general and simple method for obtaining R^2 from generalized linear mixed-effects models. *Methods in Ecology and Evolution*, 4(2), 133–142. <https://doi.org/10.1111/j.2041-210x.2012.00261.x>

- National Oceanic and Atmospheric Administration. (2006). *C-CAP land cover, Kauai, Hawaii 2005. Database: Coastal change analysis program (C-CAP) high-resolution land cover*. NOAA Office for Coastal Management. [Internet] Retrieved from https://coast.noaa.gov/htdata/raster/1/landcover/bulkdownload/hi/hi_hawaii_2005_ccap_hr_land_cover.img. Accessed December 2019.
- National Oceanic and Atmospheric Administration. (2021). Tides & currents. Retrieved from <https://tidesandcurrents.noaa.gov/noaatidepredictions.html?id=1617433>. Accessed September 2021.
- Nunn, P. D., Kumar, L., Eliot, I., & McLean, R. F. (2016). Classifying Pacific islands. *Geoscience Letters*, 3(1), 7. <https://doi.org/10.1186/s40562-016-0041-8>
- Oki, D. S. (1999). Geohydrology and numerical simulation of the groundwater flow system of Kona, Island of Hawaii. *US Geological Survey Science Investment Report*, 99–4073, 70.
- Okuhata, B. K., El-Kadi, A. I., Dulai, H., Lee, J., Wada, C. A., Bremer, L. L., et al. (2021). A density-dependent multi-species model to assess groundwater flow and nutrient transport in the coastal Keauhou aquifer, Hawai'i, USA. *Hydrogeology Journal*, 30, 1–250. <https://doi.org/10.1007/s10040-021-02407-y>
- Rohde, M. M., Froend, R., & Howard, J. (2017). A global synthesis of managing groundwater dependent ecosystems under sustainable groundwater policy. *Groundwater*, 55(3), 293–301. <https://doi.org/10.1111/gwat.12511>
- Rosado-Torres, A. A., Marino-Tapia, I., & Acevedo-Ramirez, C. (2019). Decreased roughness and macroalgae dominance in a coral reef environment with strong influence of submarine groundwater discharges. *Journal of Coastal Research*, 92(SI), 13–21. <https://doi.org/10.2112/si92-003.1>
- Sanford, T., Frumhoff, P. C., Luers, A., & Gullette, J. (2014). The climate policy narrative for a dangerously warming world. *Nature Climate Change*, 4(3), 164–166. <https://doi.org/10.1038/nclimate2148>
- Schwalm, C. R., Glendon, S., & Duffy, P. B. (2020). RCP8.5 tracks cumulative CO₂ emissions. *Proceedings of the National Academy of Sciences*, 117(33), 19656–19657. <https://doi.org/10.1073/pnas.2007117117>
- Smith, J., Smith, C., & Hunter, C. (2001). An experimental analysis of the effects of herbivory and nutrient enrichment on benthic community dynamics on a Hawaiian reef. *Coral Reefs*, 19(4), 332–342. <https://doi.org/10.1007/s003380000124>
- Smith, J. E., Brainard, R., Carter, A., Grillo, S., Edwards, C., Harris, J., et al. (2016). Re-Evaluating the health of coral reef communities: Baselines and evidence for human impacts across the central Pacific. *Proceedings of the Royal Society B*, 283(1822), 20151985. <https://doi.org/10.1098/rspb.2015.1985>
- Smith, J. E., Hunter, C. L., & Smith, C. M. (2002). Distribution and reproductive characteristics of nonindigenous and invasive marine algae in the Hawaiian Islands. *Pacific Science*, 56(3), 299–315. <https://doi.org/10.1353/psc.2002.0030>
- Smith, J. E., Hunter, C. L., & Smith, C. M. (2010). The effects of top-down versus bottom-up control on benthic coral reef community structure. *Oecologia*, 163(2), 497–507. <https://doi.org/10.1007/s00442-009-1546-z>
- Stamoulis, K. A., Friedlander, A. M., Meyer, C. G., Fernandez-Silva, I., & Toonen, R. J. (2017). Coral reef grazer-benthos dynamics complicated by invasive algae in a small marine reserve. *Scientific Reports*, 7(1), 43819. <https://doi.org/10.1038/srep43819>
- State of Hawai'i (2022). Hawai'i Statewide GIS program. Retrieved from <http://planning.hawaii.gov/gis/download-gis-data-expanded/>. Accessed July 2022.
- Tachera, D. (2021). Groundwater chemistry: Nutrient data. *Database: HydroShare*. <https://doi.org/10.4211/hs.d812bb7c93348999371c9f1f517297f>
- Taniguchi, M., Dulai, H., Burnett, K. M., Santos, I. R., Sugimoto, R., Stieglitz, T., et al. (2019). Submarine groundwater discharge: Updates on its measurement techniques, geophysical drivers, magnitudes, and effects. *Frontiers in Environmental Science*, 7, 1–26. <https://doi.org/10.3389/fenvs.2019.00141>
- Van Beukering, P. J. H., & Cesar, H. S. J. (2004). Ecological economic modeling of coral reefs: Evaluating tourist overuse at Hanauma Bay and algae blooms at the Kihei coast, Hawai'i. *Pacific Science*, 58(2), 243–260. <https://doi.org/10.1353/psc.2004.0012>
- Wada, C. A., Bremer, L. L., Burnett, K., Trauernicht, C., Giambelluca, T., Mandle, L., et al. (2017). Estimating cost-effectiveness of Hawaiian dry forest restoration using spatial changes in water yield and landscape flammability under climate change. *Pacific Science*, 71(4), 401–424. <https://doi.org/10.2984/71.4.2>
- Wada, C. A., Burnett, K. M., Okuhata, B. K., Delevaux, J. M. S., Dulai, H., El-Kadi, A. I., et al. (2021). Identifying wastewater management tradeoffs: Costs, nearshore water quality, and implications for marine coastal ecosystems in Kona, Hawai'i. *PLoS One*, 16(9), 1–26. <https://doi.org/10.1371/journal.pone.0257125>
- Wada, C. A., Pongkijvorasin, S., & Burnett, K. M. (2020). Mountain-to-sea ecological-resource management: Forested watersheds, coastal aquifers, and groundwater dependent ecosystems. *Resource and Energy Economics*, 59, 101146. <https://doi.org/10.1016/j.reseneeco.2019.101146>
- Whittier, R. B., & El-Kadi, A. I. (2009). Human and environmental risk ranking of onsite sewage disposal systems. *Final Report. Prepared for the State of Hawai'i Department of Health Safe Drinking Water Branch*. Retrieved from https://health.hawaii.gov/wastewater/files/2015/09/OSDS_OAHU.pdf
- Whittier, R. B., & El-Kadi, A. I. (2014). Human health and environmental risk ranking of on-site sewage disposal systems for the Hawaiian islands of Kauai, Molokai, and Hawaii. Final report, state Hawaii department Health, safe drinking water branch. Retrieved from https://health.hawaii.gov/wastewater/files/2015/09/OSDS_NI.pdf. Accessed 25 September 2020.
- Wickham, H. (2016). *Data analysis in: ggplot2, Use R!*. Springer. https://doi.org/10.1007/978-3-319-24277-4_9
- Williams, S. L., & Smith, J. E. (2007). A global review of the distribution, taxonomy, and impacts of introduced seaweeds. *Annual Review of Ecology, Evolution and Systematics*, 38(1), 327–359. <https://doi.org/10.1146/annurev.ecolsys.38.091206.095543>
- Wilson Okamoto Corporation. (2019). Kealahou wastewater treatment plant R-1 upgrade draft environmental impact statement. Retrieved from http://oeqc2.doh.hawaii.gov/EA_EIS_Library/2019-02-23-HA-DEIS/Kealahou-WWTP-R1-Upgrade.pdf. Accessed 15 September.
- Wright, C., Kagawa-Viviani, A., Gerlein-Safdi, C., Mosquera, G. M., Poca, M., Tseng, H., & Chun, K. P. (2017). Advancing ecophysiology in the changing tropics: Perspectives from early career scientists. *Ecophysiology*, 11(3), e1918. <https://doi.org/10.1002/eco.1918>
- Yu, C., Lee, J. A. Y., & Munro-Stasiuk, M. J. (2003). Extensions to least-cost path algorithms for roadway planning. *International Journal of Geographical Information Science*, 17(4), 361–376. <https://doi.org/10.1080/1365881031000072645>
- Zuur, A., Ieno, E. N., Walker, N., Saveliev, A. A., & Smith, G. M. (2009). *Mixed effects models and extensions in ecology with R*. Springer.